Int J Adv Manuf Technol
DOI 10.1007/s00170-017-0830-z

ORIGINAL ARTICLE

Theoretical and experimental study of slotting CFRP material with segmented helix tool

Souhir Gara[1] · **Oleg Tsoumarev**[1]

Received: 17 April 2017 / Accepted: 17 July 2017

Abstract In the present work, we studied the slotting process of carbon fiber-reinforced plastic (CFRP) material with segmented helix tool. Measurements of transverse and longitudinal surface roughness, cutting efforts, and consumed power are carried out for different combinations of cutting speed and feed per tooth in order to evaluate the influence of the cutting conditions on the machined surface quality and energy consumption. Transverse (correspondingly longitudinal) roughness refers to roughness measured perpendicular to the advance direction (correspondingly in the advance direction). Scanning electron microscope (SEM) images have been taken in order to see closely surface topography and damages that occur to the machined surface. From the results, it was found that longitudinal roughness values depend on cutting conditions which is not the case for the transverse roughness and feed per tooth makes the highest statistical and physical influence on surface roughness, cutting force, and the consumed power values. SEM images showed the presence of four different material removal mechanisms that can cause damage to the matrix or/and fibers and may generate an increase in roughness measurements.

Keywords Transverse roughness · Longitudinal roughness · Cutting force · Consumed power · Slotting · CFRP

✉ Souhir Gara
Garasouhir@yahoo.fr

[1] Laboratoire de recherche Mécanique Appliquée et Ingénierie (MAI), ENIT, Le Belvédère, BP 37, 1002 Tunis, Tunisia

Nomenclature

- R_t Total height of the roughness profile within the sampling length in micrometers
- R_a Arithmetic average roughness: the arithmetic deviation of the surface profile from the centerline in micrometers
- R_{at} Arithmetic average roughness measured in the transverse direction (perpendicular to the tool advance direction) in micrometers
- R_{al} Arithmetic average roughness measured in the longitudinal direction (in the tool advance direction) in micrometers
- R_z Ten-point height roughness: average distance between the five highest peaks and the five deepest valleys within the sampling length in micrometers
- R_{zt} Ten-point height roughness measured in the transverse direction in micrometers
- R_{zl} Ten-point height roughness measured in the longitudinal direction in micrometers
- R_y Maximum peak-to-valley height roughness: distance from the highest peak to the deepest valley within the sampling length in micrometers
- R_{yt} Maximum peak-to-valley height roughness measured in the transverse direction in micrometers
- R_{yl} Maximum peak-to-valley height roughness measured in the longitudinal direction in micrometers
- R_q Root-mean square height roughness: the root-mean square height distribution of the profile within the sampling length in micrometers
- R_{qt} Root-mean square height roughness measured in the transverse direction in micrometers
- R_{ql} Root-mean square height roughness measured in the longitudinal direction in micrometers

Published online: 17 August 2017

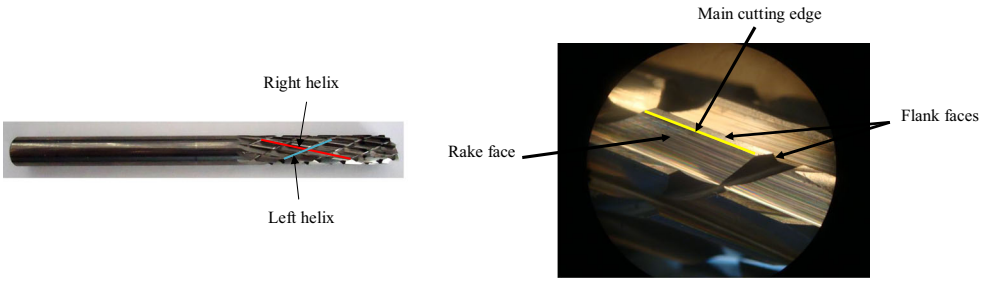

(a) *Tool* (b) *Tooth structure*

Fig. 1 Segmented helix tool. **a** Tool. **b** Tooth structure

V_c Cutting speed in meters per minute
N Spindle speed in revolutions per minute
f_z Feed per tooth in millimeters per revolution per tooth
P_c Cutting power in Watts

1 Introduction

A major difference between metallic and composite materials is their structure: isotropic for metals and anisotropic for composites. Indeed, components made from composite materials are normally cured to near-net-shape. Machining operations such as slotting, turning, drilling, edge trimming, and grinding are still required to remove excess material to final shape, produce complex contours, and meet product dimensional tolerances as well as quality surface roughness specified in the definition drawing to facilitate component assembly [1, 2].

To describe surface roughness, most research used average roughness parameter R_a [3, 4], some others choose 10-point height roughness R_z [5, 6]. Takeyama et al.[7] preferred maximum peak-to-valley height parameter R_y in order to describe machined carbon fiber reinforced plastic (CFRP) surface roughness. Gara, Wang et al. and Wern[8–10] said that R_y and R_z are better than average roughness parameter R_a and root-mean square height distribution of the profile within the sampling length R_q in quantifying the amount of surface variation in FRP materials. In 1993, Ramulu et al. [11] tried to evaluate the effectiveness of surface roughness parameters in describing the machined surface of CFRP composite: their studies have confirmed them the result of Wang et al. and Wern [9, 10]. They added that no single parameter studies can describe the surface profile measured but a combination of R_y and R_z criteria is better.

Focusing on parameters influencing surface roughness, Sheikh Ahmad et al. [12] found that transverse surface roughness does not have clear trends, it is generally higher than the longitudinal surface roughness which increased with an increase in feed rate and a decrease in spindle speed. Gara et al. [13] did not confirm this idea, they said that transverse roughness depends only on tool geometry whatever cutting condition variations when slotting of CFRP material (G803/914) with three burr tools having different geometries. Janardhan [5] said that the longitudinal roughness measurements are conditioned by tool geometry and cutting conditions: results approved by several other researchers [8, 13–17].

According to the results of the experiment, Vaclav Schornik et al. [18] found that the appropriate feed rate can be determined as 200 mm/min whereas Takeshi Yashiro et al.

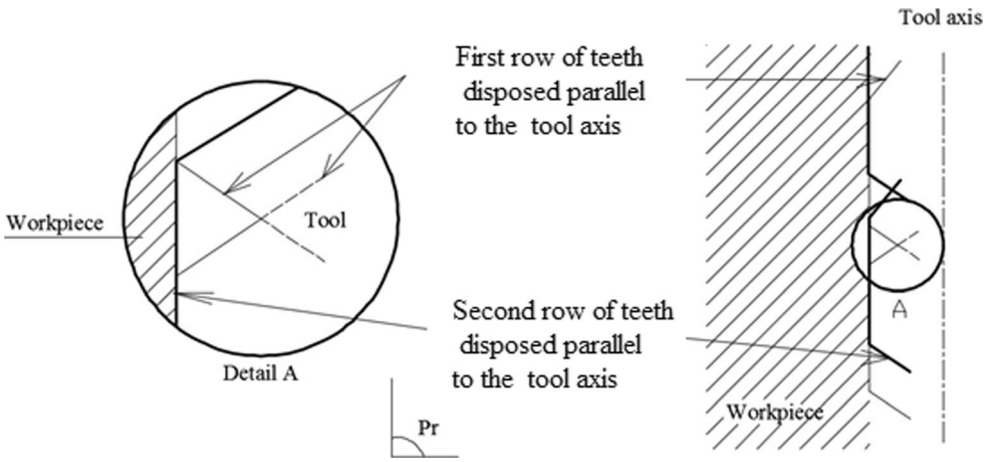

Fig. 2 Contact area segmented helix tool/workpiece

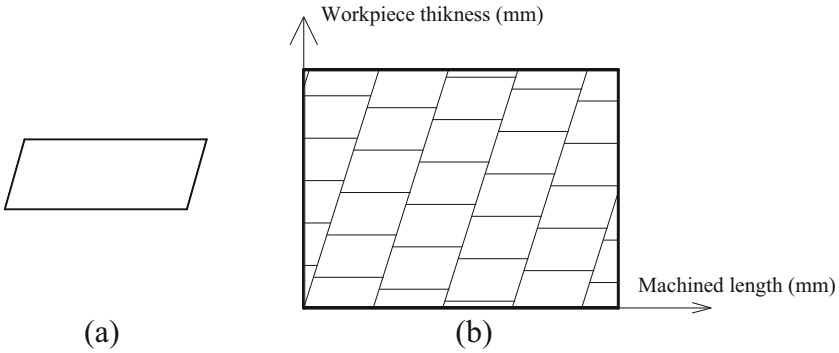

Fig. 3 Track of a tooth (**a**) and estimated topography of the machined surface (**b**)

[19] observed that the matrix resin was not influenced even if cutting speed was as high as 300 m/min within a range of variation of feed rate [75; 1500] mm/min. Puw et al. [20] added that the best surface roughness value is obtained at higher cutting speed and lower feed rate.

By studying the influence of cutting conditions on cutting forces, some researchers as Turki et al. [21] concluded that tangential cutting force increases with the increase of cutting depth and feed rate and the decrease of spindle speed. Vinayagamoorthy et al. [22] said that speed and depth of cut are factors that influence the thrust force the most while Gara et al. [23] found that feed per tooth is the key factor that has the majority impact on cutting force component values when slotting CFRP material G803/914 with burr tools. In their turn, Wang et al. [24] confirmed the idea of Gara et al. [23] and added that spindle speed influences the cutting force more than radial depth of cut.

Following an optimization study, Vinayagamoorthy et al. [22] found that (N = 1750 rpm, f_z = 0.04 mm/rev, p = 1.5 mm) are the best values of spindle speed, feed per tooth, and cutting depth to be programmed by the manufacturer when slotting composite material (manufactured by hand layup technique with isopthalic polyester as the resin and woven natural jute as the fiber) with HSS endmill. Wang et al. [24] said that (V_f = 197 mm/min; N = 1977 rpm; p = 5.68 mm) is the best combination of feed rate, spindle speed and depth of cut to be considered by an industry when machining T700/QY8911 composite plate with PCD burr tool to obtain good surface quality and high material removal rate.

The present work aims to present a theoretical model of transverse average surface roughness R_{at} and an estimated topography of slotted surface with segmented helix tool and then validate them with experimental tests: this has not been done before.

It provides also, experimental models of longitudinal surface roughness parameters, cutting forces, and consumed power for the considered tool in slotting of CFRP materials. The results will be compared with the conclusions drawn in the works of Gara et al. [13, 23] to enable us to decide on the optimal tool to be used in slotting CFRP material G803/914. The roughness criteria considered in this work are the arithmetic average roughness R_a, the 10-point height R_z, the maximum peak-to-valley height R_y, and the root-mean square height R_q.

2 Theoretical study

2.1 Tool configuration

A segmented helix tool having special design is used in his new state for tests (Fig. 1). It is a micrograin carbide tool of

Table 1 Fiber orientation material

Ply number	Orientation	Ply number	Orientation
1	0°/90°	9	0°/90°
2	45°/135°	10	45°/135°
3	0°/90°	11	0°/90°
4	45°/135°	12	45°/135°
5	45°/135°	13	45°/135°
6	0°/90°	14	0°/90°
7	45°/135°	15	45°/135°
8	0°/90°	16	0°/90°

Table 2 Physical and mechanical CFRP properties

CFRP properties	Value
Industrial reference reinforcement	G803
Industrial reference matrix	914
Minimum breaking strength	14,000 N
Minimum shear stress	60 MPa
Ply thickness	0.3 mm
Tensile strength	375 MPa
Elasticity modulus	70 GPa
Density	1500 kg/m^3

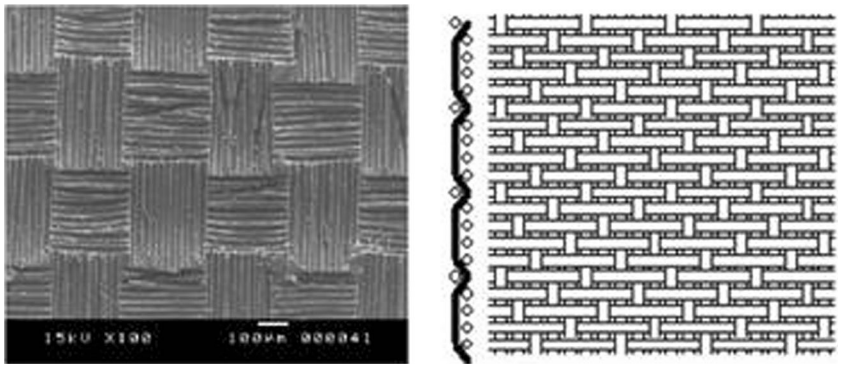

Fig. 4 CFRP laminated plate

diameter 8 mm, of overall length 100 mm, and of cutting length 45 mm. The number of its left helixes is 6 and the number of its right helixes is 12. A tooth includes one rake face, two flank faces, and linear main cutting edge.

2.2 Theoretical model of transverse roughness

Seeing of nearly the contact area tool/workpiece (Fig. 2), it can be noted that a row of teeth disposed parallel to the tool axis scrape the material left by the previous row and so on, which means that the total height of the roughness profile for the segmented helix tool is equal to:

$$R_t = 0\ \mu\text{m} \tag{1}$$

The transverse arithmetic average roughness R_{at} of a surface slotted with segmented helix tool is then given by the expression below:

$$R_{at} = 0\ \mu\text{m} \tag{2}$$

2.3 Surface topography

By looking closely at one tooth of the segmented helix tool, it appears that its shape is not standard because edges are not continuous. When the tool performs one revolution, each tooth leaves the trace given by Fig. 3a on the machined surface. During slotting operation, the teeth print their shapes on the workpiece and the machined surface will have the appearance given in Fig. 3b.

3 Experimental procedure

3.1 Method and materials

Continuous carbon fiber (referenced G803) reinforced with 42% of epoxy matrix (referenced 914) is the composite material used in tests. It was produced by manual layup of prepregs with a thickness of 0.3 mm. The fiber orientations are presented in Table 1 and the physical and mechanical properties of the CFRP laminate are given in Table 2. The plates used in the tests (Fig. 4) are 4.8 mm thick and include 16 layers. The slotting operations were carried out on a three-axis machining center SV815 SEIKI CNC AKIRA having a 30-kW spindle power, maximum spindle speed of 14,000 rpm, maximum fast feed rate of 48,000/48,000/36,000 mm/min, and advance work of 12,000 mm/min. It was equipped with a dust extraction system capable of removing fine particles.

The test specimens are mounted in a jig to make sure that vibration and displacements are eliminated. This last is fixed to a kistler force dynamometer in order to take measurements of cutting forces (Fig. 5). A three phase power sensor was used in order to measure the active power of the machine and then calculate the cutting power.

Experiments are repeated twice. At each test, measurements of consumed power and force components (F_x, F_y, and F_z), which are respectively the force along the X-direction, the feed force along the Y-direction, and the axial force along

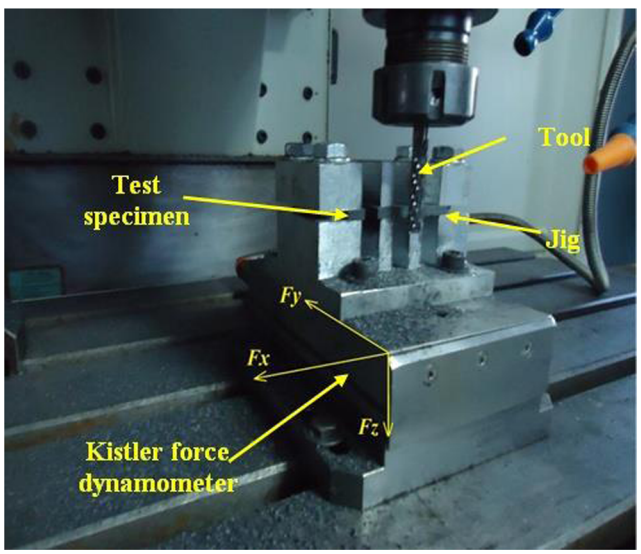

Fig. 5 Fixation of the laminate plate

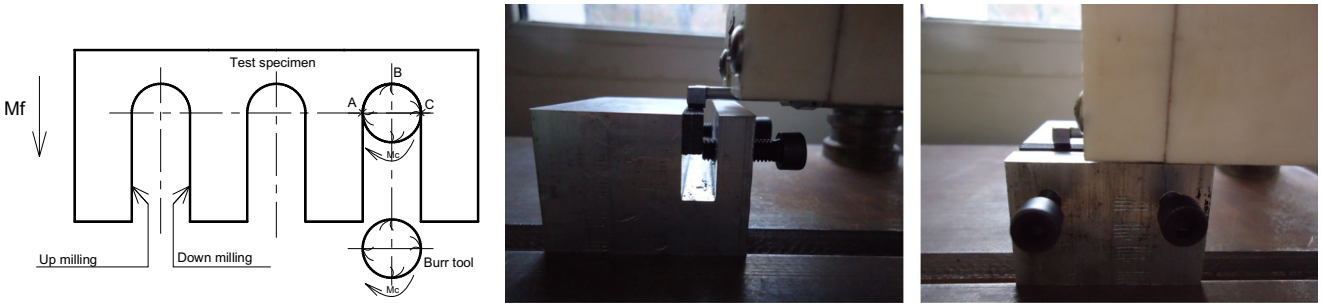

Fig. 6 **a** Slotted test specimen. **b** Mounting for measuring the transverse roughness. **c** Mounting for measuring the longitudinal roughness

the *Z*-direction (Fig. 5), are taken and results are averaged. After machining, the test specimens (Fig. 6a) are cut along the groove axis. Transverse and longitudinal average roughness are measured in up and down milling (Fig. 6b, c). SJ-201 rugosimeter was used to measure the roughness. Nine tests have been established. For each test, five measurements are made over slotted surfaces and results are averaged.

3.2 Design of experiments

In order to see which factor (cutting speed or feed per tooth) and what level of these factors will dominate longitudinal roughness measurements, cutting force components, and cutting power, a full factorial experimental design for two factors at three levels was used. This information can then be used to design more efficient experiments according to the customer requirements. Table 3 indicates the factors to be studied and the assignment allocation of the corresponding levels. The responses to be considered are longitudinal roughness parameters which are arithmetic average parameter R_{al}, 10-point height R_{zl}, maximum peak-to-valley height R_{yl}, and root-mean square height R_{ql} measured in the advance direction (perpendicular to the tool axis), cutting force components (F_x, F_y and F_z), and cutting power. The plan of experiment was made of nine tests.

4 Results and discussion

When slotting test specimens, cutting forces, and consumed power are determined and after slotting, transverse and longitudinal roughness are measured in up and down milling.

4.1 Transverse roughness

Transverse roughness parameters, which are arithmetic average R_{at}, 10-point height R_{zt}, maximum peak-to-valley height R_{yt}, and root-mean square height R_{qt}, measured perpendicular to the advance direction for the segmented helix tool, are presented in Fig. 7 which shows that Eq. 2 is validated with experimental tests because of all R_{at} values for slotted surfaces are low (they do not exceed 0.80 μm). So, it can be assumed that transverse arithmetic average roughness does not depend on cutting conditions. This result contradicts that of Sheikh Ahmad et al. [12] who found that transverse surface roughness does not have clear trends and that is generally higher than the longitudinal surface roughness and coincides with the study of Gara et al. [13] who said that transverse roughness depends only on tool geometry and not on cutting conditions when slotting composite material G803/914 with three burr tools having different geometries.

4.2 Longitudinal roughness

Figure 8 shows the results of longitudinal roughness parameters in up and down milling CFRP with segmented helix tool. It can be noted from curves that longitudinal roughness in up milling is lower than that in down milling. Comparing the founding with that of the work [13], we can say that roughness values of the surfaces slotted with the segmented helix tool are smaller than those obtained with burr tools. Moreover, the trend of variation of roughness criteria is a similar: they increase with increasing in cutting speed or/and feed per tooth. Furthermore, R_{yl} and R_{zl} are more sensitive to changes which occurred to the machined surface than R_{al} and R_{ql}, so it is better to consider R_y and R_z to describe the roughness of composites in the definition drawing.

Table 3 Assignment of the levels to the factors

Level	Factors	
	V_c (m/min)	f_z (mm/rev/tooth)
1	80	0.008
2	140	0.034
3	200	0.060

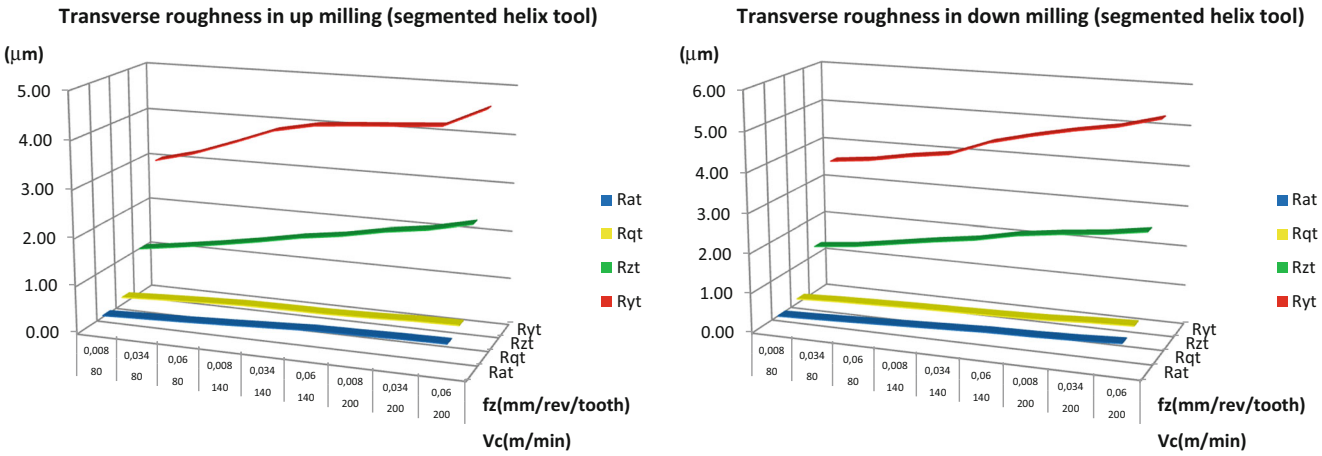

Fig. 7 Transverse roughness in selected cutting parameters (experimental results)

The plan of tests was developed in the objective of relating cutting speed and feed per tooth with longitudinal roughness parameters. The treatment of the experimental results was based on the analysis of variance (ANOVA), carried out for a level of confidence of 95% (Tables 4, 5, 6, 7), with the purpose of investigating which of the process parameters (cutting speed and feed per tooth) significantly domine longitudinal roughness. The longitudinal roughness criteria were obtained by multiple linear regression. The equations obtained are as follow:

In up milling:

$$R_{al} = 0.43 + 4.83\,x\,10^{-3}\,V_c + 27.60\,f_z \quad R = 0.99 \qquad (3)$$

$$R_{zl} = 2.11 + 1.73\,x\,10^{-2}\,V_c + 109.00\,f_z \quad R = 0.98 \qquad (4)$$

$$R_{yl} = 2.69 + 2.69\,x\,10^{-2}\,V_c + 135.00\,f_z \quad R = 0.99 \qquad (5)$$

$$R_{ql} = 0.30 + 6.42\,x\,10^{-3}\,V_c + 31.00\,f_z \quad R = 0.99 \qquad (6)$$

In down milling:

$$R_{al} = -2.10 \times 10^{-2} + 10.10 \times 10^{-3}\,V_c + 36.70\,f_z \quad R = 0.98 \qquad (7)$$

$$R_{zl} = 39.40 \times 10^{-2} + 3.80 \times 10^{-2}\,V_c + 138.00\,f_z \quad R = 0.97 \qquad (8)$$

$$R_{yl} = 0.83 + 4.97 \times 10^{-2}\,V_c + 181.00\,f_z \quad R = 0.98 \qquad (9)$$

$$R_{ql} = 21.50 \times 10^{-2} + 11.00 \times 10^{-3}\,V_c + 37.90\,f_z \quad R = 0.99 \qquad (10)$$

Being R_{al} the arithmetic average roughness in micrometers, R_{yl} the maximum peak-to-valley height in micrometers, R_{zl} the 10-point height in micrometers, and R_{ql} the root-mean square height in micrometers measured in the advance direction (perpendicular to the tool axis), V_c the cutting speed in meters per minute and f_z the feed per tooth in millimeters per revolution per tooth.

From the results of ANOVA and empirical models, it is concluded that cutting speed and feed per tooth

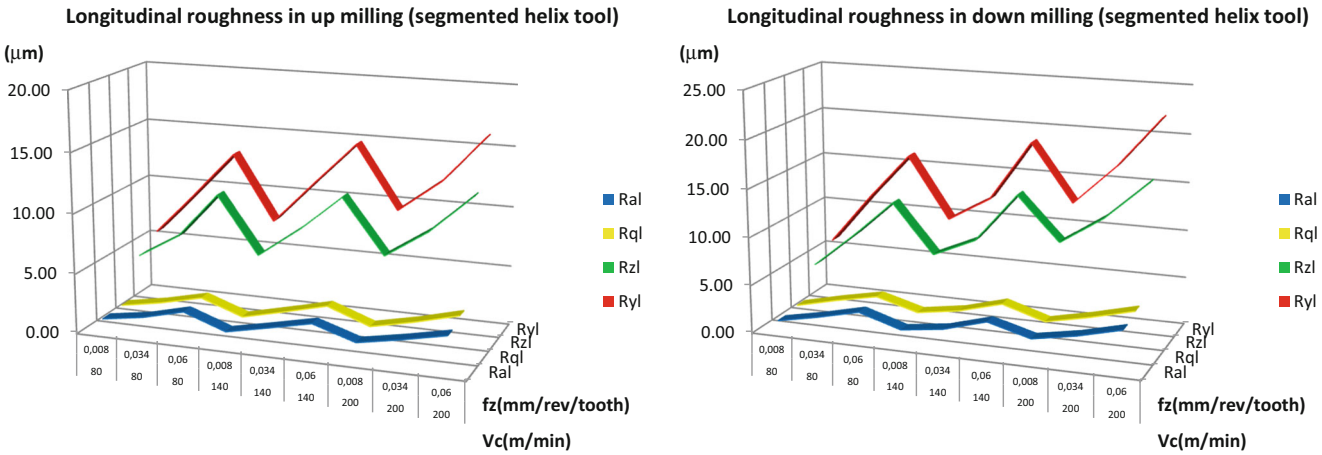

Fig. 8 Longitudinal roughness in selected cutting parameters (experimental results)

Table 4 ANOVA table for the longitudinal arithmetic average roughness R_{al} related to the segmented helix tool

Source of variance	SDQ	df	Variance	Test F	$F_{\alpha = 5\%}$	P%
Up milling						
V_c	0.51	2.00	0.25	89.51	6.94	13.81
f_z	3.11	2.00	1.55	549.33	6.94	85.56
Error	0.01	4.00	0.00	–	–	0.62
Total	3.62	8.00	–	–	–	100.00
Down milling						
V_c	2.26	2.00	1.13	176.40	6.94	28.77
f_z	5.52	2.00	2.76	431.28	6.94	70.58
Error	0.03	4.00	0.01	–	–	0.66
Total	7.81	8.00	–	–	–	100.00

SDQ sum of squares, *df* degrees of freedom, *P* percentage of contribution

Table 6 ANOVA table for the longitudinal maximum peak-to-valley height roughness R_{yl} related to the segmented helix tool

Source of variance	SDQ	df	Variance	Test F	$F_{\alpha = 5\%}$	P%
Up milling						
V_c	15.70	2.00	7.85	96.17	6.94	17.31
f_z	73.72	2.00	36.86	451.65	6.94	81.96
Error	0.33	4.00	0.08	–	–	0.73
Total	89.75	8.00	–	–	–	100.00
Down milling						
V_c	54.13	2.00	27.07	58.94	6.94	27.97
f_z	134.31	2.00	67.15	146.23	6.94	70.10
Error	1.84	4.00	0.46	–	–	1.93
Total	190.28	8.00	–	–	–	100.00

SDQ sum of squares, *df* degrees of freedom, *P* percentage of contribution

present statistical and physical significance on longitudinal roughness because $F > F_{\alpha = 5\%}$ and P (percentage of contribution) > P (error associated) especially feed per tooth.

Comparing theoretical models and experimental results (Fig. 9), it appears clearly that Eqs. 3–10 follow the evolution of roughness criteria with an acceptable approximation.

4.3 Cutting forces

The variation of the cutting forces as a function of cutting conditions during slotting composite laminate plate of industrial reference G803/914 are summarized in Table 8. It shows that:

- Cutting forces decrease with the increase in cutting speed: this is due to the augmentation in cutting temperature and thus the weakening of the structure of the workpiece material: this finding has been presented in the work [5, 21, 23, 24].
- Cutting forces increase with increasing in feed per tooth: this is due to the increase of the cutting section: this result was found by the researchers [5, 21, 23, 24].

An analysis of variance of the data was done in order to investigate which of the parameters (cutting speed and feed per tooth) dominate the cutting force components the most.

Table 9 shows the results of the ANOVA with three cutting force components generated in slotting of CFRP material with

Table 5 ANOVA table for the longitudinal 10-point height roughness R_{zl} related to the segmented helix tool

Source of variance	SDQ	df	Variance	Test F	$F_{\alpha = 5\%}$	P%
Up milling						
V_c	6.46	2.00	3.23	60.58	6.94	11.52
f_z	48.47	2.00	24.23	454.51	6.94	87.70
Error	0.21	4.00	0.05	–	–	0.77
Total	55.14	8.00	–	–	–	100.00
Down milling						
V_c	31.82	2.00	15.91	71.89	6.94	28.26
f_z	78.33	2.00	39.17	176.98	6.94	70.15
Error	0.89	4.00	0.22	–	–	1.59
Total	111.04	8.00	–	–	–	100.00

SDQ sum of squares, *df* degrees of freedom, *P* percentage of contribution

Table 7 ANOVA table for the longitudinal root-mean square height roughness Rql related to the segmented helix tool

Source of variance	SDQ	df	Variance	Test F	$F_{\alpha = 5\%}$	P%
Up milling						
V_c	0.89	2.00	0.45	66.51	6.94	18.16
f_z	3.91	2.00	1.96	292.20	6.94	80.73
Error	0.03	4.00	0.01	–	–	1.11
Total	4.83	8.00	–	–	–	100.00
Down milling						
V_c	2.64	2.00	1.32	111.15	6.94	30.65
f_z	5.85	2.00	2.92	246.26	6.94	68.24
Error	0.05	4.00	0.01	–	–	1.11
Total	8.53	8.00	–	–	–	100.00

SDQ sum of squares, *df* degrees of freedom, *P* percentage of contribution

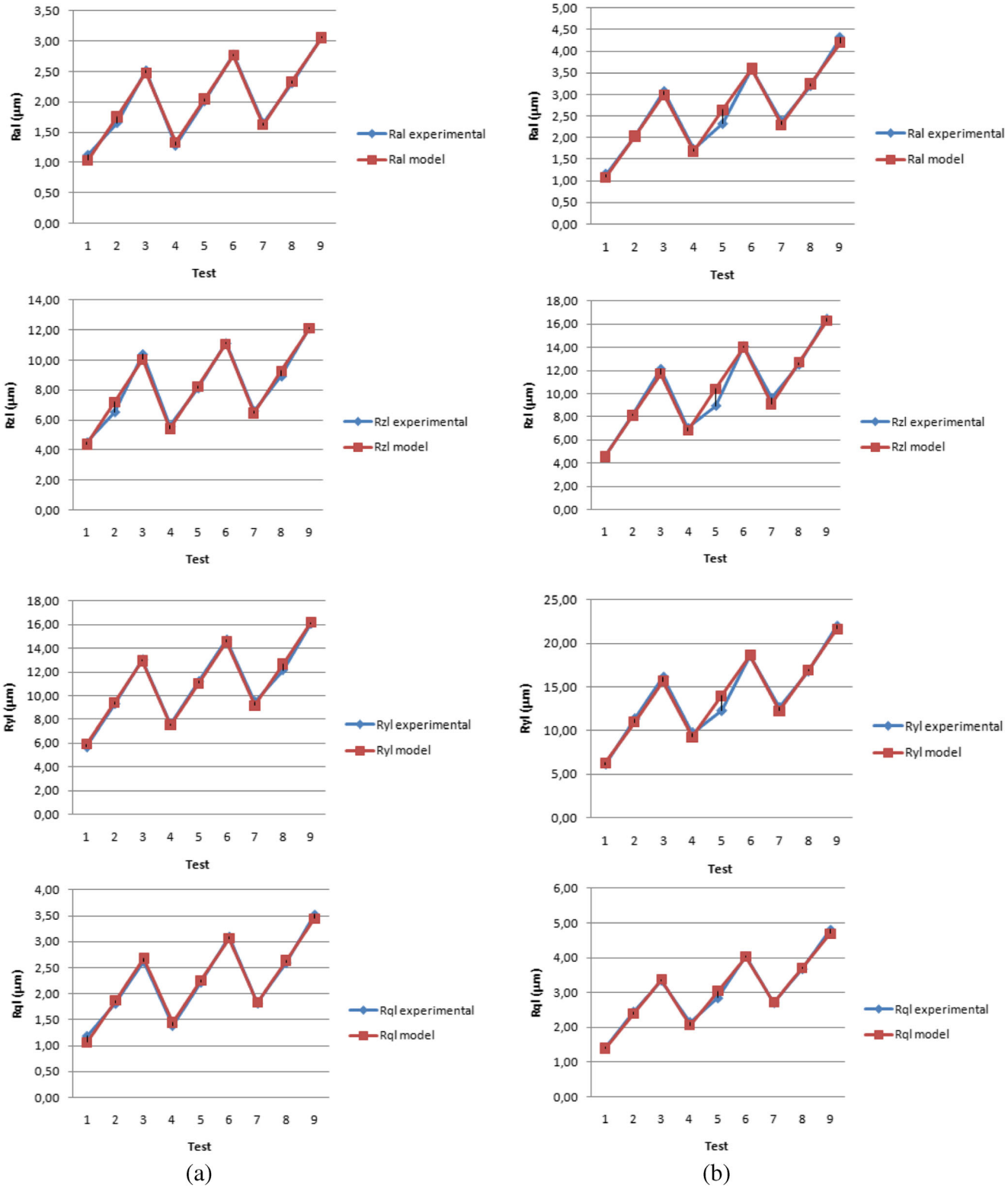

Fig. 9 Comparison of experimental data and theoretical models in **a** up milling and **b** down milling

segmented helix tool. This analysis was carried out for a level of confidence of 95%.

From Table 9, it can be found that, feed per tooth is the factor that present statistical and physical significance on the three force components the most because $F > F_{\alpha\ =\ 5\%}$ and P (percentage of contribution) > P (error associated). This result was established by the researchers [5, 21, 23, 24].

Table 8 Values of cutting forces as a function of cutting parameters

Test	V_c (m/min)	f_z (mm/ rev/tooth)	F_x (N)			F_y (N)			F_z (N)		
			Test 1	Test 2	Average	Test 1	Test 2	Average	Test 1	Test 2	Average
1	80	0.008	106.20	108.31	107.26	328.86	327.10	327.98	6.25	6.36	6.31
2	80	0.034	124.57	127.10	125.84	346.04	344.02	345.03	12.10	11.17	11.64
3	80	0.060	135.66	137.57	136.62	365.02	363.80	364.41	17.86	17.28	17.57
4	140	0.008	101.56	101.34	101.45	318.34	315.61	316.98	5.27	5.31	5.29
5	140	0.034	120.08	121.39	120.74	332.50	330.61	331.56	9.76	10.47	10.12
6	140	0.060	130.08	128.39	129.24	353.80	351.48	352.64	14.34	15.64	14.99
7	200	0.008	94.55	96.62	95.59	298.96	295.04	297.00	4.98	4.86	4.92
8	200	0.034	115.26	112.55	113.91	307.32	308.69	308.01	8.22	8.73	8,48
9	200	0.060	124.12	126.33	125.23	338.25	339.20	338.73	13.86	12.41	13.14

The three cutting force components generated in slotting of CFRP material with segmented helix tool were obtained by multiple linear regression. The resulting equations are presented in the following expressions:

$$F_x = 112,000 - 0.097\,V_c + 556\,f_z \quad R = 0.97 \tag{11}$$

$$F_y = 343,000 - 0.260\,V_c + 730\,f_z \quad R = 0.97 \tag{12}$$

$$F_z = 7.410 - 0.025\,V_c + 187\,f_z \quad R = 0.98 \tag{13}$$

By comparing theoretical models and experimental results (Fig. 10), we can say that Eqs. 11–13 correlate the evolution of cutting force components function of cutting speed and feed per tooth with reasonable degree of approximation.

4.4 Cutting power

Power measurements are given by a wattmeter connected to the variable speed drive of the machine. The curves obtained give the value of the power absorbed during the slotting operation. Figure 11 shows an example and the cutting power P_c is determined from the expression below:

$$P_c = P_{measured} - P_0 \tag{14}$$

Being P_{measured} as the measured power and P_0 as the no-load power (power before machining) in Watts.

The values of the cutting power calculated from the expression 14 of the two replicas tests are summarized in Table 10.

Table 9 ANOVA table for the cutting forces related to the segmented helix tool

Source of variance	SDQ	df	Variance	Test F	$F_{\alpha = 5\%}$	P%
F_x						
V_c	204.19	2.00	102.10	175.68	6.94	13.55
f_z	1291.80	2.00	645.90	1111.45	6.94	86.14
Error	2.32	4.00	0.58	–	–	0.31
Total	1498.31	8.00	–	–	–	100.00
F_y						
V_c	1487.63	2.00	743.81	77.55	6.94	39.36
f_z	2204.42	2.00	1102.21	114.92	6.94	58.58
Error	38.36	4.00	9.59	–	–	2.06
Total	3730.41	8.00	–	–	–	100.00
F_z						
V_c	13.53	2.00	6.76	11.25	6.94	7.80
f_z	142.08	2.00	71.04	118.17	6.94	89.16
Error	2.40	4.00	0.60	–	–	3.04
Total	158.01	8.00	–	–	–	100.00

SDQ sum of squares, *df* degrees of freedom, *P* percentage of contribution

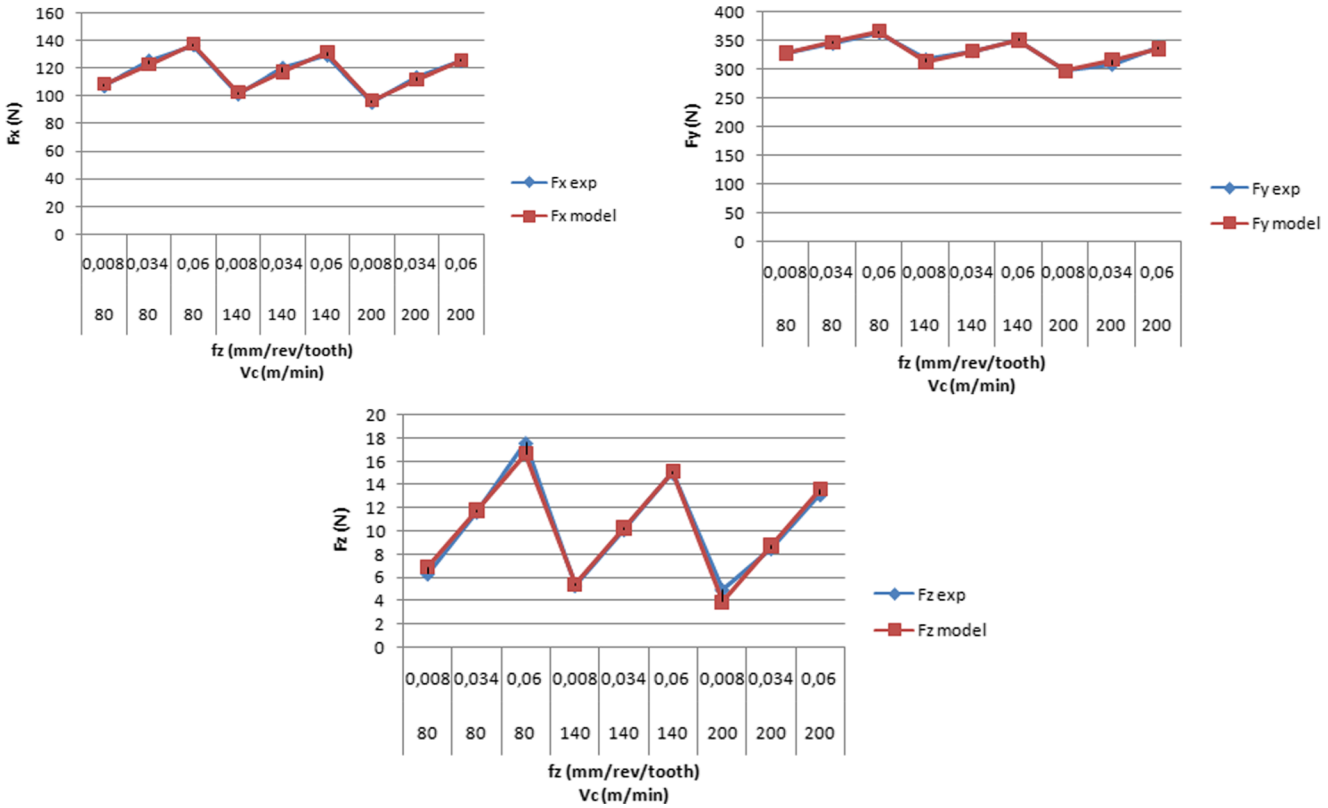

Fig. 10 Comparison of experimental data and theoretical models (cutting efforts)

Table 11 shows the results of the ANOVA with cutting power consumed in slotting of CFRP material with segmented helix tool. This analysis was carried out for a level of confidence of 95%.

From Table 11, it can be found that feed per tooth present statistical and physical significance on cutting power more than cutting speed. This result was established by the researchers [5, 21, 24].

The cutting power was obtained by multiple linear regression. The resulting equation is defined by the expression:

$$P_c = -0.232 + 3.600 \times 10^{-3} V_c + 8.690 f_z \quad R = 0.97 \quad (15)$$

The evolution of Eq. 15 and the experimental results of consumed power function of cutting speed and feed per tooth coincide approximately (Fig. 12).

4.5 Analysis of the machined surface

Observations on a scanning electron microscope (SEM) have been established and have enabled us to note the presence of four chip removal mechanisms (Fig. 13), namely:

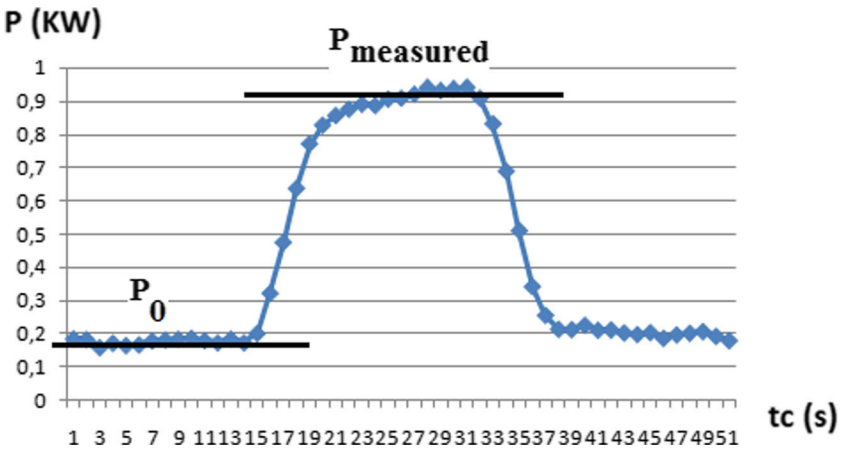

Fig. 11 Power curve (V_c = 200 m/min, f_z = 0.034 mm/rev/tooth)

Table 10 Values of cutting power as a function of cutting parameters

Test	V_c (m/min)	f_z (mm/rev/tooth)	P_c (KW)		
			Test 1	Test 2	Average
1	80	0.008	0.200	0.190	0.195
2	80	0.034	0.342	0.340	0.341
3	80	0.060	0.511	0.500	0.506
4	140	0.008	0.340	0.342	0.341
5	140	0.034	0.582	0.575	0.579
6	140	0.060	0.800	0.817	0.809
7	200	0.008	0.482	0.490	0.486
8	200	0.034	0.800	0.780	0.790
9	200	0.060	1.100	1.025	1.063

- Mechanism 1: the machined surface appears as packets. In fact, following the first contact between a tooth and the slotted surface, an interfacial rupture occurs between the fiber and the matrix. By advancing, a rupture of portions of fiber and matrix occurs perpendicularly to the longitudinal fiber axes.
- Mechanism 2: from the first contact between the tool and the machined surface, a tooth exerts pressure on fiber and matrix. Following the advance and cutting movement, the intensity of the force increases. If its value reaches the shear limit of the fibers, they will be cut perpendicular to their longitudinal axes; otherwise, they will change orientation and remain glued to the surface.
- Mechanism 3: by contacting the workpiece during a slotting operation, a tooth exerts pressure on the fibers and the matrix, which may cause compression or microbuckling stresses depending on the orientation of the fibers. This effect generates the fragmentation or/and cracks of some fibers.
- Mechanism 4: when contact between the tool and the material occurs, degradation of the fiber/matrix interface happens due to the stress intensity and the important cutting temperature. This effect can generate changes in resin structure and then in the resin shape and appearance even if glass transition temperature is not reached.

Table 11 ANOVA table for the cutting power related to the segmented helix tool

Source of variance	SDQ	df	Variance	Test F	$F_{\alpha=5\%}$	P%
V_c	0.28	2.00	0.14	31.23	6.94	44.92
f_z	0.31	2.00	0.15	34.06	6.94	49.13
Error	0.02	4.00	0.00	–	–	5.94
Total	0.61	8.00	–	–	–	100.00

SDQ sum of squares, *df* degrees of freedom, *P* percentage of contribution

SEM images show residual resin scraped off by the teeth of the tool (Fig. 14). By comparing it with respect to Fig. 3b, it can be stated that the estimated topography of the machined surface is validated whatever the chip removal mechanism and cutting condition values.

5 Conclusion

The work focuses on measurements of surface roughness, cutting efforts, and cutting power during slotting of CFRP material referenced G803/914 with segmented helix tool. The correlation of cutting conditions, tool geometry, and machined surface was examined in order to have an idea about what is happening in the contact area tool/workpiece. Based on the presented results, the following conclusions are drawn:

1. Transverse roughness criteria (R_{at}, R_{zt}, R_{yt}, and R_{qt}) have the same trend of evolution, they do not depend on cutting conditions: it is sufficient to study a single parameter in order to describe CFRP machined surface quality in the transverse direction.
2. Longitudinal roughness criteria (R_{al}, R_{zt}, R_{yt}, and R_{ql}) depend on cutting conditions: the average roughness and the root-mean square height parameters are less sensitive to surface changes than the maximum peak-to-valley height and the 10-point height in the longitudinal direction: it is not sufficient to study single parameter in order to describe the surface profile in the longitudinal direction (R_{yl} and R_{zl} are better than R_{al} and R_{ql}). Moreover, longitudinal roughness in up milling is lower than that in down milling.
3. Eqs. 3–10 obtained can be effectively used to evaluate the slotted CFRP surface roughness with the segmented helix tool. Feed per tooth presents the highest statistical and physical influence on surface roughness.
4. By comparing this work with that of Gara et al. [13], it can be stated that knurled tool design influence radically the surface roughness measurements: the segmented helix tool gives minimum surface roughness values when slotting of CFRP, it leaves better combination between resin and fiber and receives less damage after machining the same cutting length than the burr tool. It is the suitable tool to choose from the manufacturer if he opted to work by fixing the objective “minimum machined surface roughness value”.
5. Eqs. 11–13 and 15 obtained can be used to evaluate cutting force components and the cutting power in slotting CFRP material with the segmented helix tool. Feed per

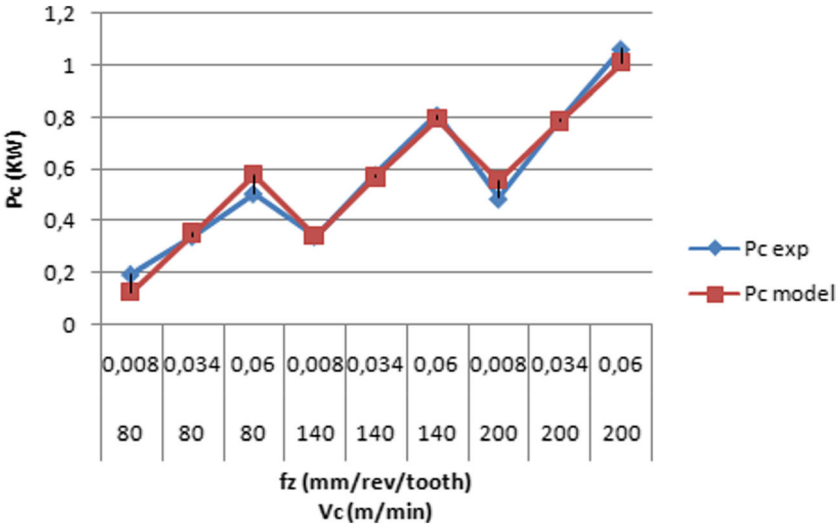

Fig. 12 Comparison of experimental data and theoretical models (cutting power)

tooth presents the highest statistical and physical influence on cutting forces and power.

6. By comparing this work with that of Gara et al. [23], it can be noted that the segmented helix tool gives minimum resulting cutting force than burr tools when slotting of CFRP. It is the suitable tool to choose from the manufacturer if he opted to work by fixing the objective "minimum resulting cutting force value".

An optimization of cutting conditions in slotting of CFRP material (G803/914) with segmented helix tool considering the criteria: roughness lower than that recorded in the

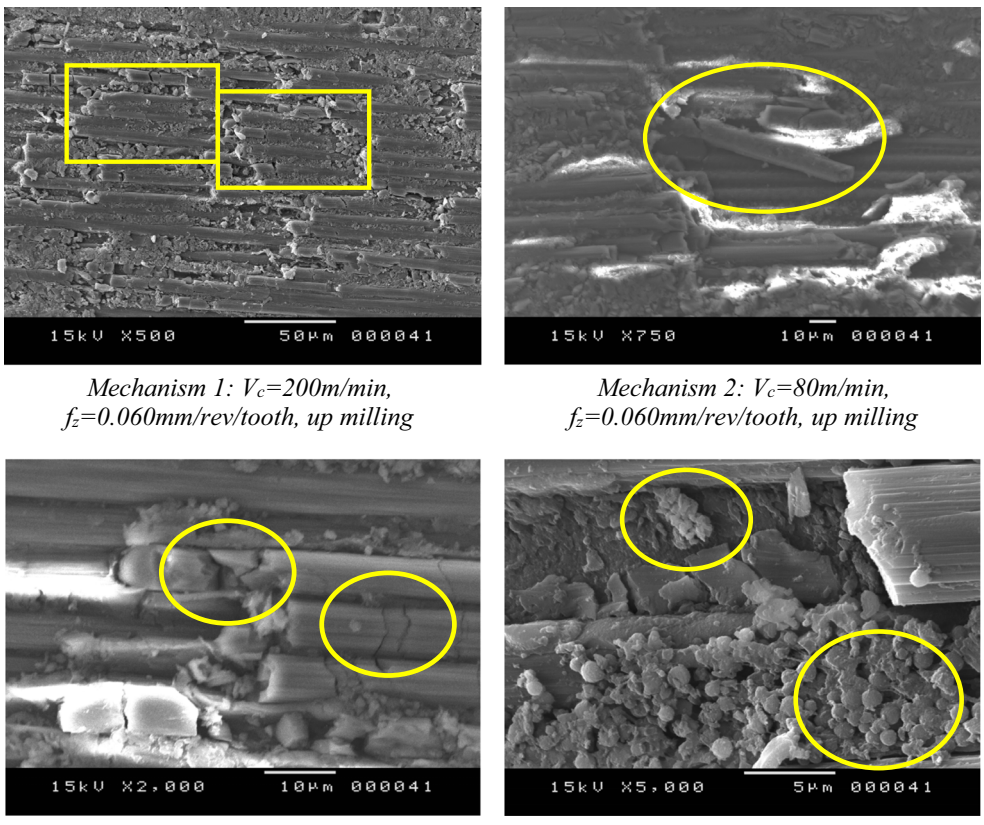

Mechanism 1: V_c=200m/min, f_z=0.060mm/rev/tooth, up milling

Mechanism 2: V_c=80m/min, f_z=0.060mm/rev/tooth, up milling

Mechanism 3: V_c=80m/min, f_z=0.008mm/rev/tooth, up milling

Mechanism 4: V_c=200m/min, f_z=0.008mm/rev/tooth, up milling

Fig. 13 SEM images of CFRP surfaces slotted with segmented helix tool

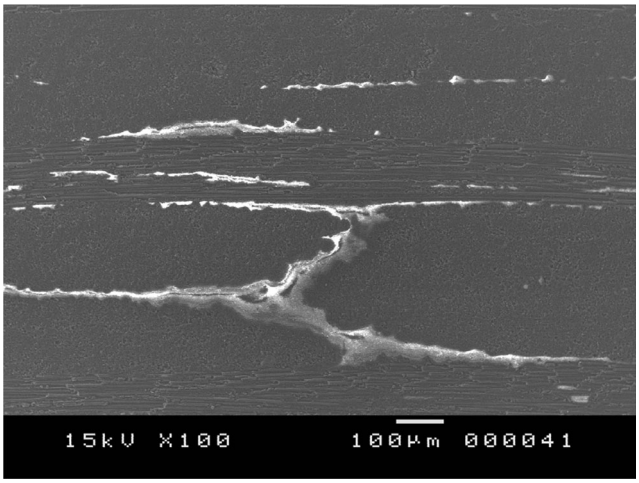

Fig. 14 Surface topography (V_c = 80 m/min, f_z = 0.008 mm/rev/tooth, up milling)

definition drawing, temperature lower than the glass transition temperature, minimum cutting forces, maximum removal rate, and minimum cutting specific energy will be investigated.

Acknowledgements The authors acknowledge the Higher Institute of Technological Studies of Nabeul, the National School of Engineers of Monastir and the National School of Engineers of Tunis for allowing us to use their equipment in the experimental work.

References

1. El-Hofy MH, Sooa SL, Aspinwalla DK, Simb WM, Pearsonc D, Hardend P (2011) Factors affecting workpiece surface integrity in slotting of CFRP. Procedia Engineering 19:94–99
2. Hocheng H, Puw HY and Huang Y (1993) Preliminary study on milling of unidirectional carbon fibre-reinforced plastics, Composites Manufacturing Vol. 4 No 2
3. Paulo Davim J, Reis P (2005) Damage and dimensional precision on milling carbon fiber-reinforced plastics using design experiments. J Mater Process Technol 160:160–167
4. Ghidossi Patrick (2003) Contribution à l'étude de l'effet des conditions d'usinage d'éprouvettes en composites à matrice polymère sur leur réponse mécanique, thesis, ENSAM
5. Janardhan Prashanth. Tool wear of diamond interlocked tools in routing of CFRP composites, thesis, Faculty of the graduate school of Wichita State University, December 2005
6. Konig W, Grab P (1989) Quality definition and essessment in drilling of FRP thermosets. Annals of CIRP 38(1):119–124
7. Takeyama H, Iijima N (1988) Machinability of glass fiber reinforced plastics and application of ultrasonic machining. Annals of CIRP 37(1):93–96
8. Gara S. (2016) Approche théorique et expérimentale du détourage d'un composite en carbone/époxy moyennant des fraises à dentures croisées, thesis, Ecole Nationale d'ingénieurs de Tunis, Tunisia
9. Wang DH, Ramulu M, Wern CW (1992) Orthogonal cutting characteristics of graphite/epoxy composite materials. Trans NAMRI/SME 20:159–165
10. Wern CW (1991) Surface characteristics of machined graphite/epoxy composite, MS thesis, University of Washington
11. Ramulu M, Wern CW, Garbini JL (1993) Effect of the direction on surface roughness measurements of machined graphite/epoxy composite. Compos Manuf 4(1):39–51
12. Jamal SA, Urban N, Cheraghi H (2012) Machining damage in edge trimming of CFRP. Mater Manuf Process 27:802–808
13. Gara S, Tsoumarev O (2015) Effect of tool geometry on surface roughness in slotting of CFRP. Int J Adv Manuf Technol. doi:10.1007/s00170-015-8185-9
14. Durao Luis MP, Magalhaes AG, Marques AT, Baptista AM, Figueiredo M (2008) Drilling of fiber reinforced plastic laminates, Materials Science Forum, vol 587–588. Trans Tech Publications, Switzerland, pp 706–710
15. Durao Luis MP, Gonçalves DJS, Tavares JMRS, Albuquerque VHC, Marques AT, Baptista AM (2010) Drilling of carbon fiber reinforced laminates- a comparative analysis of five different drills on thrust force, roughness and delamination, Materials Science Forum, vol 636–637. Trans Tech Publications, Switzerland, pp 206–213
16. Gonçalves Daniel JS, Durao Luis MP, Tavares Joao Manuel RS, Albuquerque VHC, Torres Marques A (2010) Evaluation of tools and cutting conditions on carbon fibre reinforced laminates, Materials Science Forum, vol 638–642. Trans Tech Publications, Switzerland, pp 944–949
17. Vijay Kumar N, Gokul Nathan G, Krishnaraj V, Sasidharan G (2013) Effect of tool geometry in drilling of aerospace materials, Int J Sci Eng Res, 4(8)
18. Schornik V, Dana M, Zetkova I (2015) The influence of the cutting conditions on the machined surface quality when the CFRP is machined. Procedia Eng 100:1270–1276
19. Takeshi Y, Takayuki O, Hiroyuki S (2013) Temperature measurment of cutting tool and machined surface layer in milling of CFRP. Int J Mach Tool Manuf 70:63–69
20. Puw HY, Hocheng H (1998) Chip formation model of cutting fiber-reinforced plastics perpendicular to fiber axis. J Manuf Sci Eng 120(1):192–196
21. Turki Y, Habak M, Velasco R, Vantomme P, Aboura Z (2011) Etude expérimentale du détourage d'un composite carbone/époxy, 17ème colloque national de la recherche dans les IUT, CNRIUT, 8–10 june. Cherbourg-Octeville, France
22. Vinayagamoorthy R, Rajeswari N (2012) Analysis of cutting forces during milling of natural fibered composites using fuzzy logic. Int J Compos Mater Manuf 2(3):15–21
23. Gara S, Ramzi Fredj, Sami Naîmi and Oleg Tsoumarev (2016) Prediction of cutting forces in slotting of multidirectional CFRP laminate, Int J Adv Manuf Technol, DOI 10.1007/s00170-016-9161-8
24. Wang H, Sun J, Li J, Lu L, Li N (2016) Evaluation of cutting force and cutting temperature in milling carbon fiber-reinforced polymer composites. Int J Adv Manuf Technol 82(9):1517–1525